LJMU Research Online

Sadique, MM, Al-Nageim, H, Atherton, W, Seton, L and Dempster, NM

 Analytical investigation of hydration mechanism of a non-Portland binder with waste paper sludge ash

http://researchonline.ljmu.ac.uk/id/eprint/10961/

Article

http://researchonline.ljmu.ac.uk/

Analytical investigation of hydration mechanism of a non-Portland binder with waste paper sludge ash

Monower Sadique[1], Hassan Al-Nageim[2], William Atherton[3], Linda Seton[4], Nicola Dempster[5]

[1] Senior Lecturer, Department of Civil Engineering, Liverpool John Moores University Byrom Street, Liverpool, L3 3AF, UK, Email: M.M.Sadique@ljmu.ac.uk; sadiquerhd@hotmail.com

[2] Professor, Department of Civil Engineering Liverpool John Moores University
[3] Principal Lecturer, Department of Civil Engineering Liverpool John Moores University
[4] Senior Lecturer, Pharmacy and Biomolecular Sciences, Liverpool John Moores University
[5] Senior Research Officer, Pharmacy and Biomolecular Sciences, Liverpool John Moores University,

Abstract: The development and production of new materials requires advanced analytical characterisation to explain the relation between the physico-chemical structure of the material and its properties. Highly integrated microelectronic structure analysis of surfaces with laser beams and x-ray fluorescence aided devices are found to be helpful for providing important information, including the interrelationships between physical, chemical, mechanical and durability characteristics of the new developed products. In most instances no single technique provides all the needed information and hence simultaneous application of several techniques becomes necessary. This study was aimed for hydration analysis, characterization and evaluation of a new novel non-Portland binder (NPB) with waste paper sludge ash (PSA) using FTIR and TG/DTA. The progressive formation of hydration products within the non-Portland binder was identified and their microstructural characteristics were analysed. The stable and non-expansive nature of secondary ettringite formation was also identified after a period of 365 days curing.

Key words: Non-Portland binder; waste paper sludge ash, FT-IR; TG/DTA

1. Introduction:

One of the most significant current discussions in the construction sector is the reduction of carbon emission from its production and application process. The supplementary cementitious material (SCM) plays a key role in achieving this objective. Different types of additions other than the standard listed materials such as calcined clay, sewage sludge ash, rice husk ash, wood ash, sugar cane bagasse ash, corn cob ash, kaolin waste, perlite,

diatomite, air pollution control residue, etc have been studied as SCM. Much of the research up to now has been concluded by activating the additions with ordinary Portland cement (OPC) and/or ground granulated blast furnace slags (GGBS) and so far there has been little discussion about cement and GGBS free systems [1-10].

Advancement has been achieved by using wet milled paper sludge ash (PSA) with GGBS (PSA: GGBS, 50:50) in cement free systems [11]. However attention should also be given concerning curing, reinforecement cover and carbonation when the GGBS level is more than 50% [12]. Moreover GGBS is no longer classified as a waste and hence there is increasing concern regarding the replacement of GGBS with other waste/s such as SCM.

At the same time, the development and production of new materials requires advanced analytical characterisation to explain the relation between the physico-chemical structure of the material and its properties. Highly integrated microelectronic structure analysis of surfaces with laser beams and x-ray fluorescence aided devices are found to be helpful for analysing substances at micro and molecular level [13]. In addition to characterization, they provide important information, including the interrelationships between physical, chemical, mechanical and durability characteristics of the developed products. In most instances no single technique provides all the needed information and hence simultaneous application of several techniques becomes necessary.

Different experimental techniques have been employed by researchers to investigate the chemical and morphological reaction upon hydration. The application of XRD, DTA and SEM to track changes in hydrated phases during the hydration process has been suggested by various authors [14-16]. A combined XRD/TG/DTA analysis has been suggested as a valuable means in order to develop a better understanding of the hydration phenomenon by Esteves [17]. This is because different techniques utilise different operating principles and hence a simultaneous application of them will be expected to provide multi-dimensional information of the hydration products of a binder. As a result, irrespective of the crystal or amorphous characteristics of the hydrates, chemical and morphological status can be obtained.

A new novel non-portland binder (NPB) was developed through synergistic physico-chemical composition by using PSA (60%) and blending it with another alkali sulphate-rich bio mass fly ash (20%) and silica fume (20%) and gypsum aided grinding. This study was aimed for investigating the hydration mechanism, characterization and evaluation of the new novel NPB using analytical techniques.

2. Materials and experimental procedure

2.1 Materials

The chemical and physical properties of the new NPB and control cement have been provided in Table 1. For analysis and comparison with new NPB, a commercially available Portland composite cement type CEM-II/A/LL 42.5-N has been used in this study which contains between approximately 6% to 20% limestone.

Table 1: Physico-chemical properties of new NPB and control cement

	CEM-II	NPB	PSA	Bio mass fly ash	SF
D_{50}, μm	13.3	10.6			
Fineness (BET), m^2/gm	6.78	9.67			
Density, gm/cm^3	3.05	2.59			
Soundness (mm) [BS EN requirement<10mm]	1.3	2.0			
Initial setting time(min) [BS EN requirement>60min]	150	70			
Pozzolanicity (at 15 day)	Positive	Positive			
Loss on Ignition, %	1.45	14.3			
Na_2O	1.5	1.8	2.0	3.5	1.0
CaO	62.58	45.15	57	20.5	-
SiO_2	25.06	31.19	28	15.8	97.0
Al_2O_3	2.26	3.49	3.7	-	-
SO_3	1.92	3.5	0.3	13.3	-
Cl	-	0.5	-	-	-
K_2O	0.75	4.00	-	18.8	-
Na_2O-equ [%]	*2.0*	*4.2*			

2.2 Fourier transform-infrared spectroscopy (FT-IR)

Generally, infrared is used for the determination of molecular structure, identification of compounds, and quantitative/qualitative determination of phase composition. At the same time, it is possible to detect not only crystalline but also the amorphous phases developed by cementitious materials, mainly at early ages, by using this tool [18]. In this study, the spectrum of the sample was recorded by accumulating 16 scans at 4 cm^{-1} resolution between 515 cm^{-1} and 4000 cm^{-1} using a Perkin-Elmer Spectrum BX series Fourier transform infrared spectrometer (FT-IR) equipped with a MIRacle ATR accessory (Specac, UK), as shown in

Figure 3.3 (a). The samples were finely ground for one minute, combined with pre-dried spectroscopic grade KBr (containing approximately 0.5% wt sample) and pressed into a disc under 10 tonnes of pressure (as shown in Figure 3.3b), following the process mentioned in previous studies [19-21].

2.3 Thermal analysis

Thermal analysis has been defined by the International Confederation of Thermal Analysis (ICTA) as a general term which covers a variety of techniques that record the physico-chemical changes occurring in a substance as a function of temperature [22]. Two common complimentary techniques in this category are differential scanning calorimetry (DSC) and thermo gravimetric analysis (TGA). DSC measures heat flow to or from a sample as a function of temperature and time and TGA continuously measures the weight of a sample as a function of temperature and time. Differential thermal analysis (DTA) is a method similar to DSC, where the difference in temperature between the sample and a reference material is recorded while both are subjected to the same heating programme. For assessing the moisture and volatility, decomposition kinetics and composition thermo gravimetric analysis is widely used whereas DTA is used to determine the presence of exothermic or endothermic reactions. In this study, a Perkin Elmer TGA7 analyser was used to analyse the binder paste and LOI of different materials by simultaneous TG/DTA. The samples were heated in a tungsten crucible at a constant rate of 5°C/min using inert nitrogen gas in the temperature range from 24°C to 960°C. Commercial software Pyris was used to quantify the mass loss and identify the peaks from TGA and DTA. The changes in sample weight indicate material loss and phase transformation that occurs at particular temperatures.

2.4 Specimen for molecular and thermal investigation

For analysing hydration kinetics, phase development and microstructural analysis, the paste specimens of the NPB and control cement were prepared at a water/binder ratio of 0.50 and cured at 20°C under water and analysed at designated ages. There are similarities between the approach followed in this study and those described by Singh [23] and Tkaczewska [24]. The mortar specimens of NPB using the optimised design parameters (binder:sand ratio of 1:2.25, water/binder ratio of 0.45 with 1.5% SP) were prepared and cured for up to 90 days. The comparative strength development between NPB and the control cement (cement:sand ratio of 1:2.25 and water/cement ratio of 0.35) is displayed in

Figure 1. Though NPB shows slightly lower early strength than the control, however, its rate of hydration was more than that of the control between 7 days and 28 days. However, the increase in strength after 28 days was very low in NPB compared to that of the control mortar.
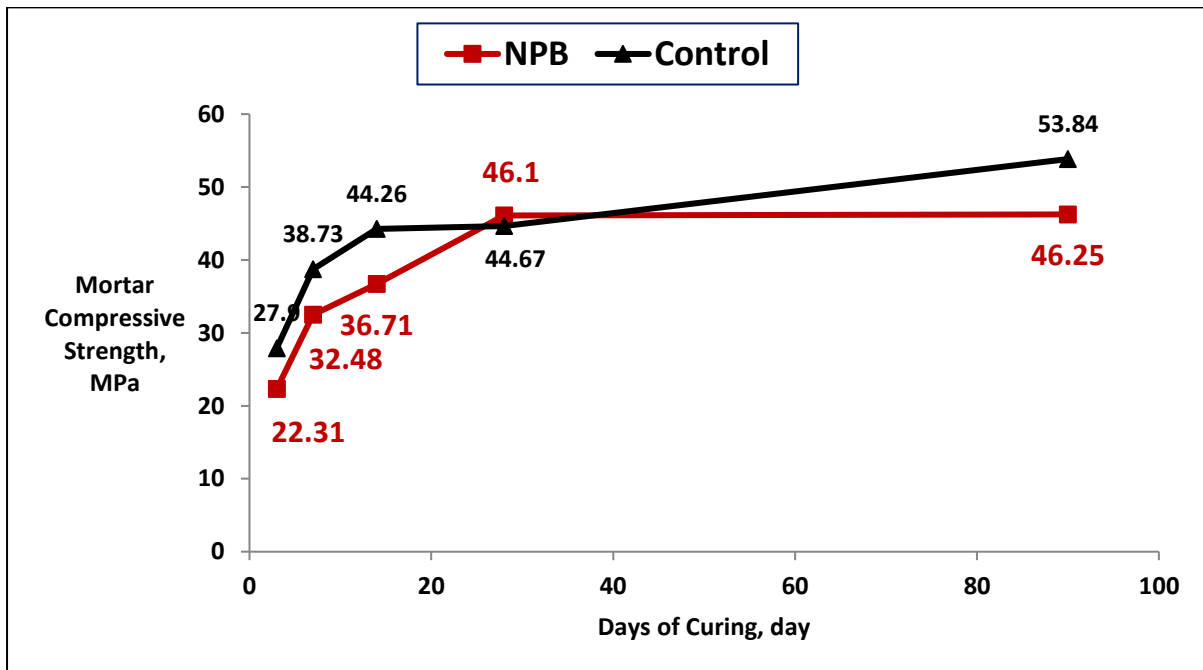

Figure 1: Optimised strength development by NPB and reference cement mortar

3. Results and discussion

3.1 Analysis of hydrates by TG/DTA

Thermal analysis techniques such as DTA and TG have been used to study the hydration kinetics, mechanism of hydration and estimation of hydration products [15]. Differential thermal analysis (DTA) combined with thermogravimetric analysis (TGA) was identified by Pane et al. [25] as a more suitable technique for studying hydration. This technique has been widely used by various researchers in the hydration of clinkerless cement [26] as well as binary and ternary blended cement containing different SCMs [27-30], in addition to its use in pure cement hydration [31]. A TG instrument records the thermally activated events by measuring the temperature and associated weight of the sample. These data provide various information regarding moisture content, oxidation or decomposition temperatures which are then correlated for the presence of different compound/s. DTA locates the ranges

corresponding to thermal decompositions of different phases in the paste, while TGA simultaneously measures the weight loss due to the decompositions. The TG/DT analysis of NPB paste ranging from 7 days to 1 year was conducted and is shown in Figure 2. A different temperature range for identifying the hydration products from interpreting the TG/DTA curve was suggested by various researchers and a summary of these interpretations is shown in Table 2.

Table 2: Review of interpretation of TG/DTA curve for identifying hydration products

Temperature range	Comments
150° C [17] 115°C - 225°C [22] 95°C [30]	Endothermic peak is attributed to the de-hydroxylation, dehydration of CSH phase
120°C - 130° C [22] 165°C [32]	Endothermic peak is attributed to the de-hydroxylation of Ettringite (AFm) phase
410°C [17] 430°C – 550 °C [22] 350°C – 550 °C [33] 465°C – 470 °C [32] 465°C – 470 °C [30]	Mass loss due to the decomposition of $Ca(OH)_2$ or portlandite
750°C - 850 °C [22] 550°C - 800 °C [33]	Decomposition of $CaCO_3$

To avoid interference by non-reacted residual water, at designated periods the hardened paste was dried at 20°C for four hours before TGA following a simplest method as suggested by [30] . Based on the suggestion provided by previous studies (as shown in Table 2), the findings from the TG/DTA profile for NPB (as plotted in Figures 2) are summarised in Table 3. The thermogram for the reference cement paste is plotted in Figure 3. The absolute mass loss increases with age (up to 28 days) were evident from Figure 1 and Table 3. This was an indirect indication of degree of hydration within the ternary blend and was in accordance with the result stated by Esteves [17] in the case of plain cement and silica fume modified cement.
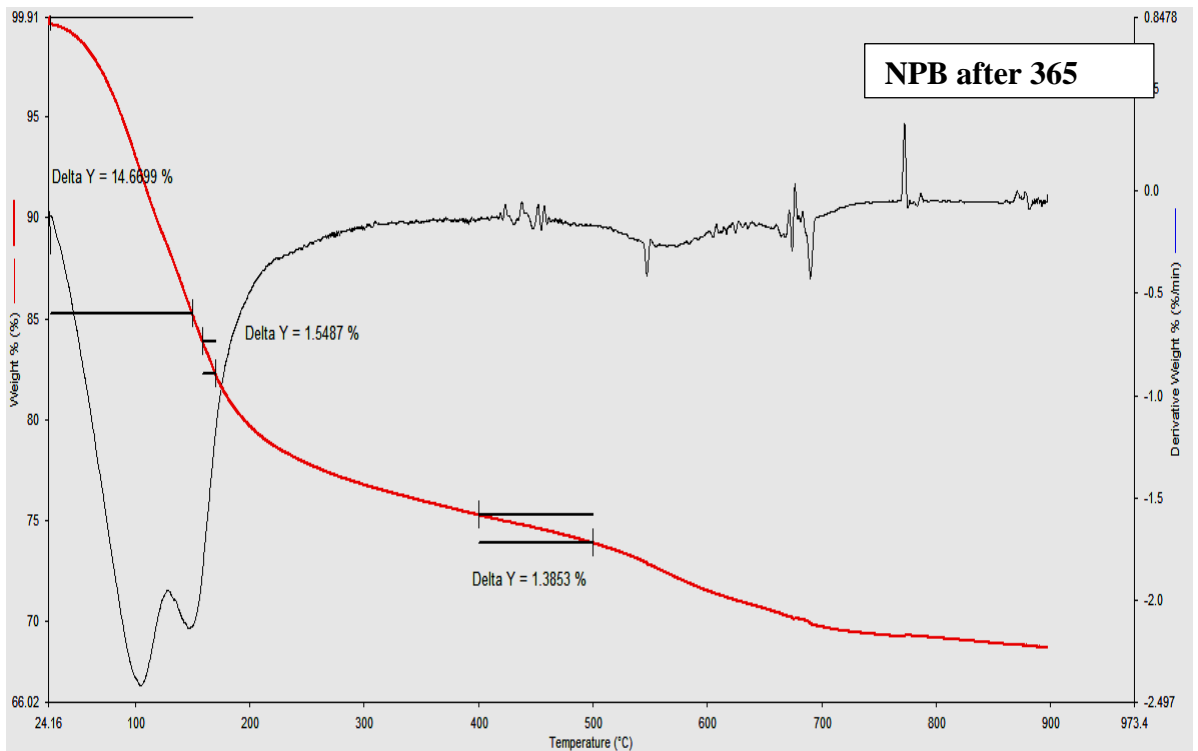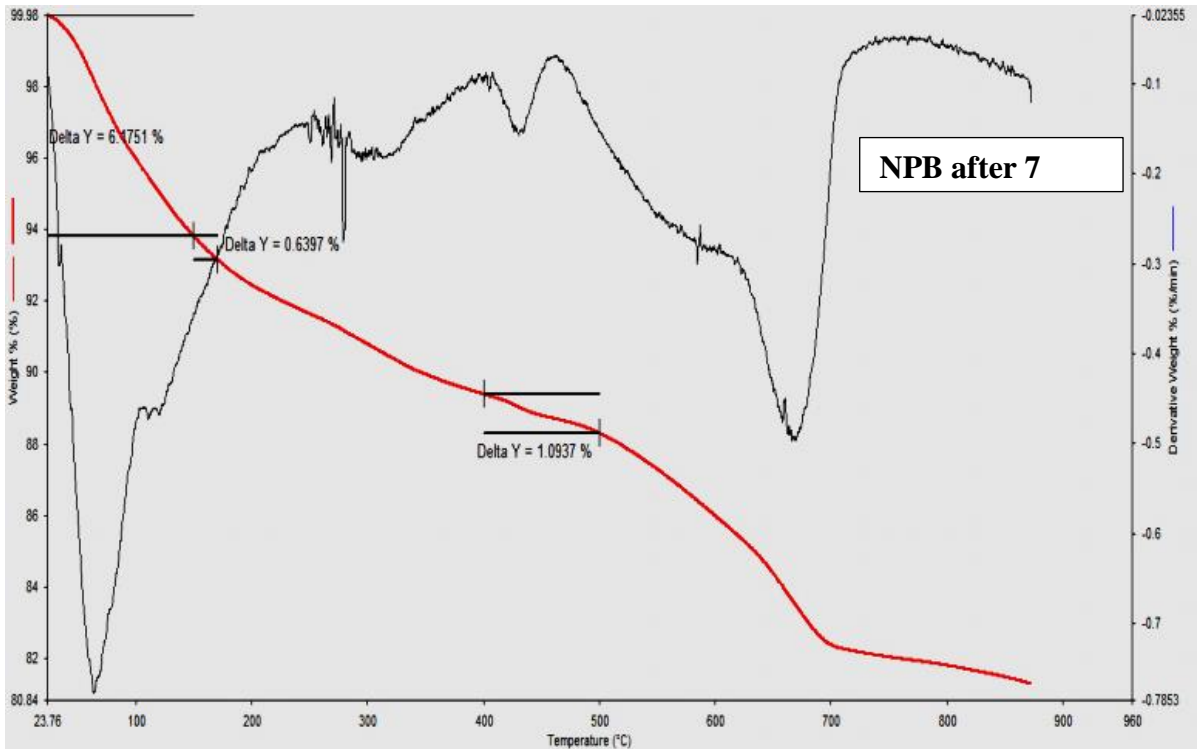
Figure 2: Thermogram of NPB after 7 and 365 days curing

Table 3: Summary of TG/DTA curve for NPB paste

Temperature range	Comments	% Mass loss				
		7 day	14 day	28 day	90 day	365 day
0-150° C	Endothermic peak is attributed to the de-hydroxylation of CSH phase	6.17	22.43	25.49	23.30	14.6
150- 170° C	Mass loss is attributed to the de-hydroxylation of Ettringite (AFm) phase	0.63	0.76	0.78	0.95	1.5
400 – 500 °C	Mass loss due to the dehydration of $Ca(OH)_2$ or portlandite (C-H)	1.0	0.78	0.98	1.6	1.3
Absolute mass loss (%)		20	35	37	35	32

Moreover, based on the results presented in Table 3, it is evident that the mass loss in the temperature interval 0-150°C with the first strong endothermic peak was attributed to de-hydroxylation of CSH and found to be increasing until 28 days of curing. The main weight loss in this stage is due to the loss of weakly bound water on the gel solid, which was physically adsorbed, and is taken at about 90-110°C. Furthermore, the appearance of a new exothermic peak at 790°C without a significant mass change was due to recrystallisation of C-S-H [20] and was found to be related to pozzolanic activity of silica fume within the NPB[17]. The increased mass loss and shifting of DTA peaks towards higher temperature with increase of hydration age was due to the formation of C-S-H further, which supports the idea of Kourounis et al. [34]. The second major endothermic peak at 7 days of hydration and the corresponding mass loss in TG curve at 400-500°C, as shown in Figure 2, corresponds to the dehydration of the CH phase, formed for further hydration through the reaction of silicate with water. Similar thermal analysis was also reported in a recent work by Esteves [17] for a cement-silica fume system.

The reduction of endothermic peak intensity at 400-500°C with ages in the case of the NPB and reference cement (as shown in Figures 2 and 3) indicates the dropping densities of C-H crystal for Pozzolanic reaction, since the increase of DTA peak with age was attributed for denser and larger C-H crystal, as has been reported in a previous study [32]. The consumption of C-H by PFA for hydration reaction and, as a consequence, the disappearance of the DTA peak was also reported in work by Escalante et al. [35]. At the same time the DTA peak at 110°C, which was attributed to AFt at 7 days, was found to be consumed (disappearance of peak) with ages and converted to AFm, that has been ensured by the new peak appeared at 150°C after one year. The presence of stronger AFt peak with increased mass loss (Table 2) and reduction of C-H peak intensities indicate that the Pozzolanic reaction within the new NPB and the reference cement was in agreement with the results reported by Escalante [35] for the ternary system of gypsum-OPC-PFA. During hydration, soluble K^+ will rapidly increase the pH and accelerate hydration, which will be expected to be balanced by SO_4^{2-} [36]. During hydration, immediately upon the interaction of NPB with water, ionic species from alkali sulphate (K^+, Na^+ and SO_4^{2-}) within alkali sulphate-rich fly ash dissolute in the liquid phase due to high solubility and form hydrates. Higher solubility and rapid solution of gypsum (GA) make the concentration of SO_4^{2-} ions reach the saturation point immediately in water. Similar kinetics was reported by Fu et al. [37], while using 5% gypsum with sulphoaluminate cement clinker. Thus, the formation of C-S-H, portlandite [$Ca(OH)_2$], ettringite [($Ca_6Al_2(SO_4)_3(OH)_{12} \cdot 26H_2O$] and alunite [$KAl_3(SO_4)_2(OH)_6$] by reactive silica with arcanite of alkali suphate reach fly ash and soluble calcium and aluminium of PSA is more evident in the ternary blend prepared with GA assisted ground fly ashes. A high ratio of SO_4^{2-} to available $Al(OH)_4$ from the aluminate phase favours the formation of ettringite (AFt) [38]. Moreover, potassium alunite in XRD was also detected by Katsioti et al. [36] when replacing cement with 20% alunite. Quick dissolution of K^+ and Na^+ ions from their sulphates into the liquid phase has also been suggested by Odler [16]. At the same time $CaSO_4$ (from GA) dissolves and contributes Ca^{2+} and additional SO_4^{2-} ions until saturation. The aluminate containing oxides of PSA dissolve at this stage and react with Ca^{2+} and SO_4^{2-} and precipitate as ettringite or as AFt phase. On the progression of hydration, due to a shortage of SO_4^{2-} ions as a consequence of complete dissolution of $CaSO_4$, the previously formed ettringite (AFt) phase is converted to monosulphates ($C_3A.CaSO_4.12H_2O$) [16]. The nucleation of the calcium silicate hydrate (C-S-H) phase is also initiated at this stage. Moreover, silica fume synthesis promotes pozzolanic reaction with calcium hydroxide and

alkaline hydroxides, thereby forming a C-S-H. The C-S-H phase continues to be formed for on-going hydration. The presence of C–S–H, ettringite, monosulfate aluminate and calcium hydroxide in the hardened mixtures confirmed that hydration reactions within the NPB had occurred. The rate of formation of C-S-H with the advancement of Pozzolanic reaction through consuming C-H by silica fume was very high up to 28 days and formed a dense compacted hydration product. This observation from thermal analysis was consistent with the strength development profile by the blend shown in Figure 1.
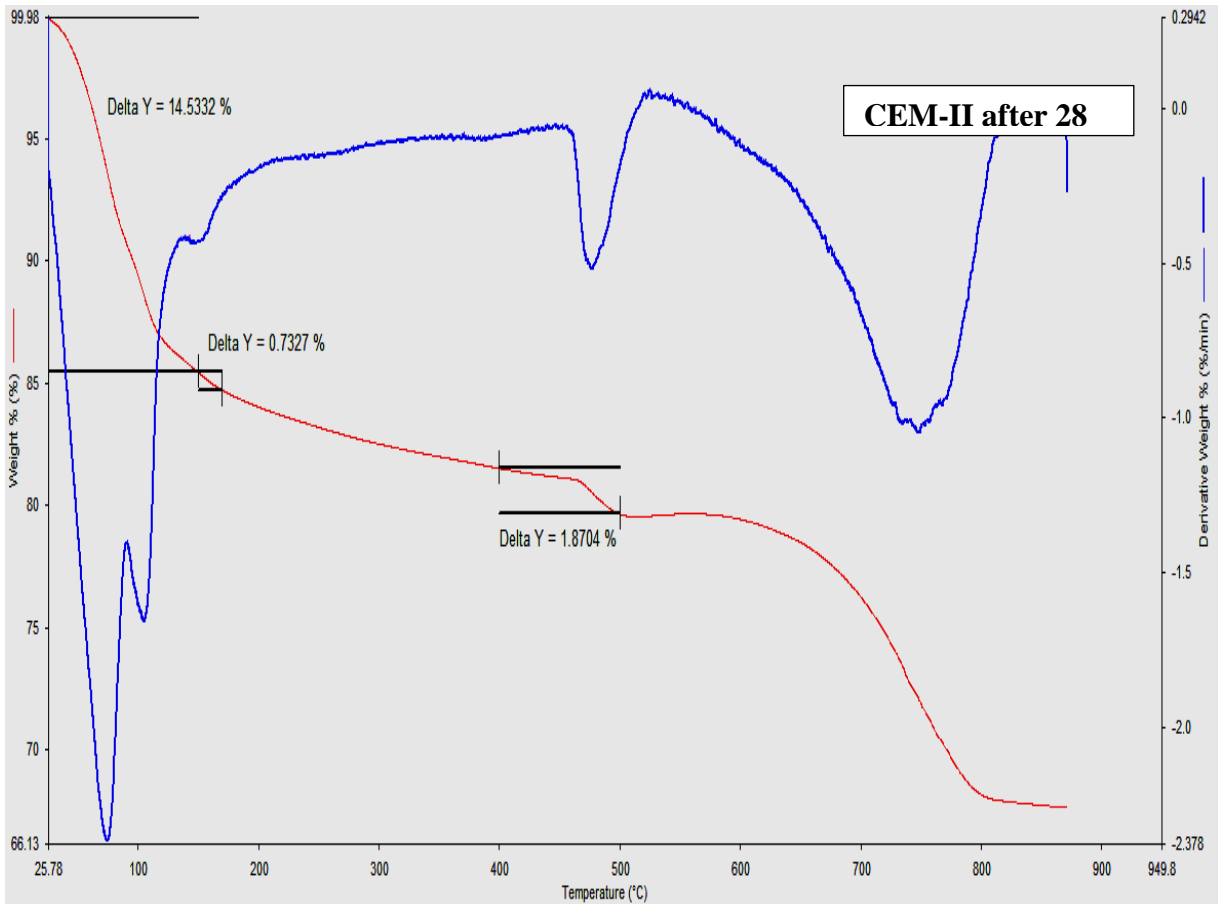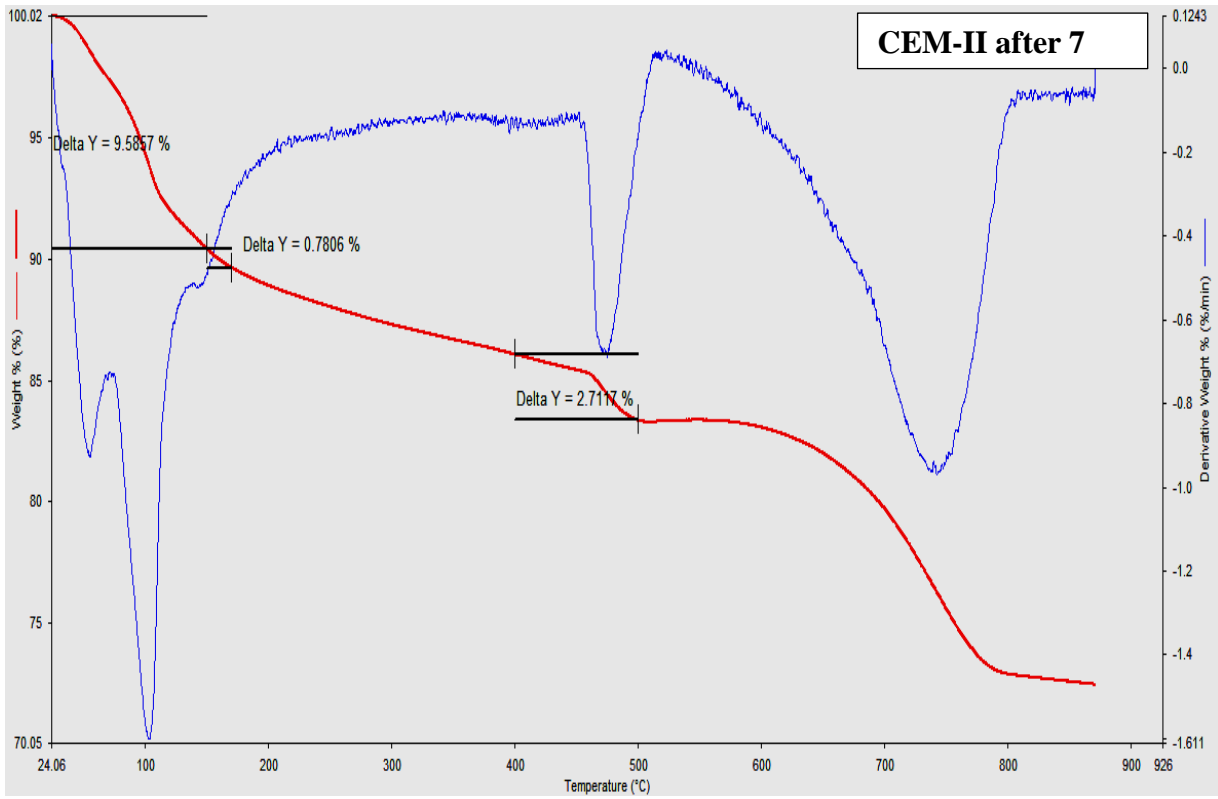
Figure 3: Thermogram of the reference cement after 7 and 28 days curing

3.2 Analysis of hydrates by FT-IR

The identification of the main hydration product of blended cement [20] and pure cement [18] using FT-IR in association with IR spectral characteristics during the progress of hydration has been studied previously. The progressive hydration was found to be accompanied by the increase of the intensities of C-S-H absorption bands and simultaneous decrease of absorption bands of constituent minerals [39]. The IR spectral studies of hydration of NPB and control cement paste with increasing ages have been plotted in Figure 4 and Figure 5 respectively. For identifying the successive changes in constituent materials and hydration products, the absorption band of anhydrous (powder) NPB and control cement have also been inserted in the IR spectrum of hydrated pastes in Figure 4 and Figure 5 respectively. For comparing the IR absorption band of hydrated paste in detail, only the spectrum of early hydration at 1 day of NPB has been plotted in Figure 6.

The IR spectra of ettringite presents a very strong band centered towards 1120 cm^{-1}. However, considerable difference between the spectra of two types of calcium sulfoaluminate hydrates AFm and AFt phases, in association with identification of a very strong characteristic band at 1100 cm^{-1} and 1120 cm^{-1} respectively was reported by Bensted et al. [40]. At the same time, early formation of ettringite on hydration was shown by a change in the sulphate absorption to a singlet centred at 1120 cm^{-1}, and the subsequent replacement of ettringite by monosulfate by a further return to a doublet at 1100 and 1170 cm^{-1} was stated by Taylor [38]. Hence the strong singlet absorption peak for AFt at 1117 cm^{-1} after 1 day (Figure 6) and initiation of return of doublet at 7 days and the subsequent appearance of a strong doublet for conversion of AFt to AFm at 1113 cm^{-1} and 967 cm^{-1} after 28 day (Figure 4) in the case of NPB was in accordance with Taylor's observation. In the case of control paste, the appearance of a doublet for AFm was identified at 1113 and 981 cm^{-1} after 28 days (Figure 5). This observation was also in accordance with the findings from thermal analysis reported in the previous section. The presence of a strong C-H absorption band at 3641 cm^{-1} and AFt band at 1118 cm^{-1} after 1 day (Figure 6) of curing were the main early strength generating elements for NPB that have been confirmed by the observed compressive strength of 22.31MPa after 3 days (Figure 1). Previous studies reported that, during sulphate activation, the increased SO_4^{2-} concentration reacts with the alumina phase in fly ash and forms aluminosulphate which combines with Ca^{2+} and forms ettringite. This ettringite contributes strength at an early stage [41-43]. Moreover, the main products of hydration, C-S-H, were

12

detected in the IR spectra from the absorption band at 965-975 cm^{-1} [39], 1428 cm^{-1}, 3420 cm^{-1} [18].

Subsequently, progressive increases in the intensity of the absorption band of C-S-H with age at 1415 cm^{-1} and 1420 cm^{-1} (as shown in Figure 4 and Figure 5) played a dominating role for generating strength within the NPB and control mortar respectively, which continued up to 90 days. The changes that occurred in the H$_2$O bending band near 1650 cm^{-1} and in the H$_2$O or OH stretching bands at 3100-3700 cm^{-1} also confirm the successful hydration within the ternary blend [38]. Moreover, the consumption of portlandite for progressive hydration and diminishing C-H band subsequently at 3630 cm^{-1} with age was also found to be in agreement with the TG/DTA observation of NPB paste.
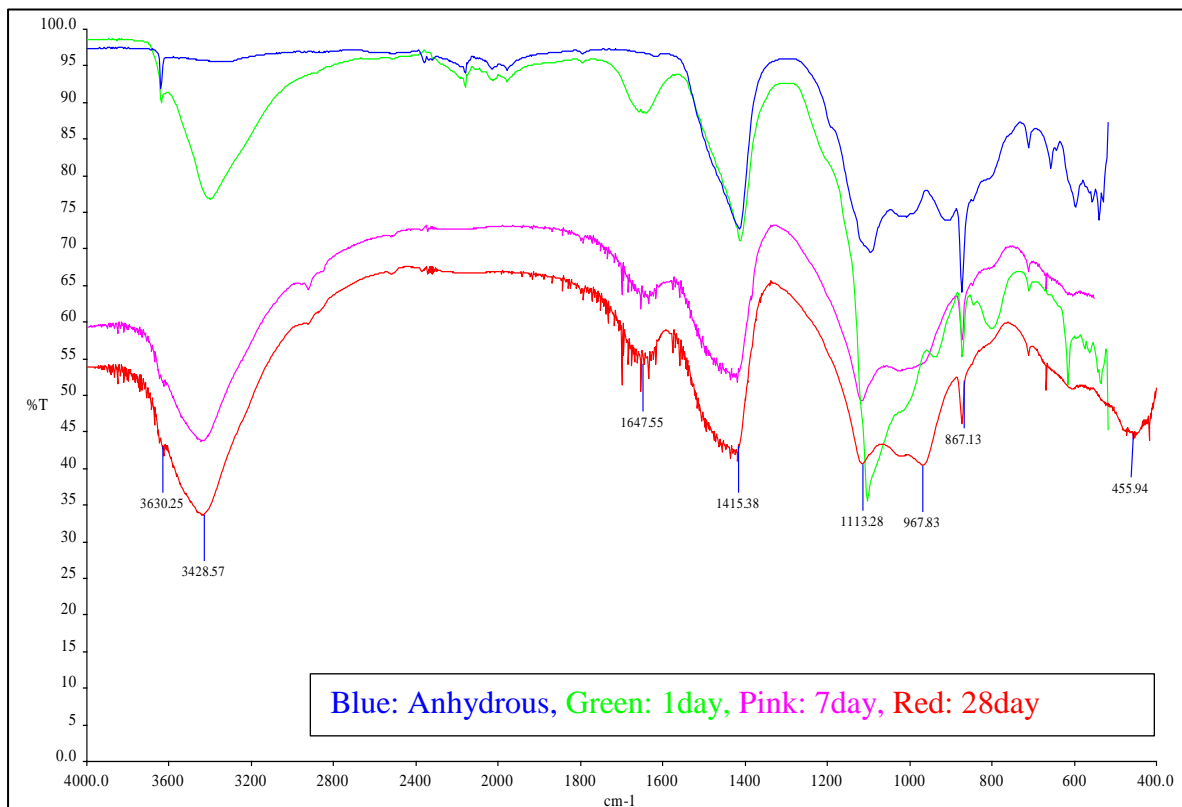

Figure 4: FT-IR spectra for hydrated paste and anhydrous powder of NPB
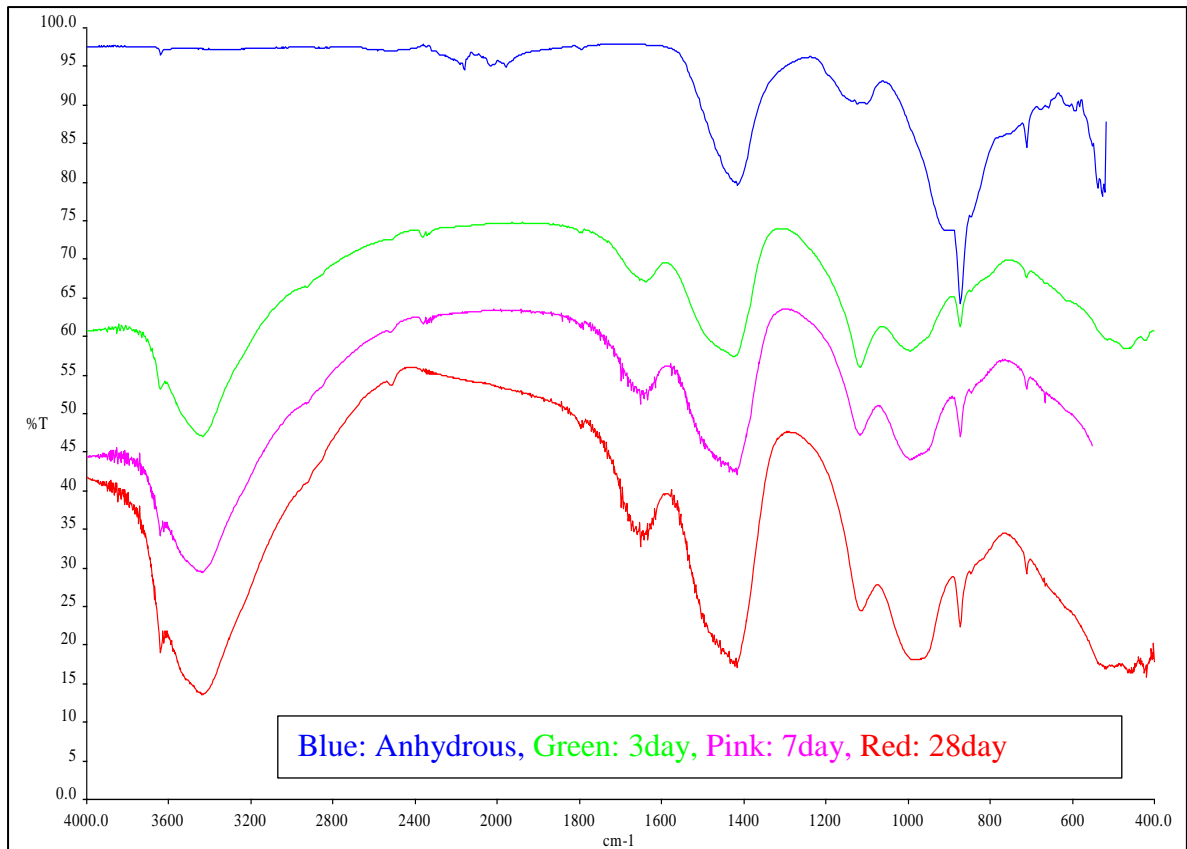
13

Figure 5: FT-IR spectra for hydrated paste and anhydrous powder of control cement

Blue: Anhydrous, Green: 3day, Pink: 7day, Red: 28day
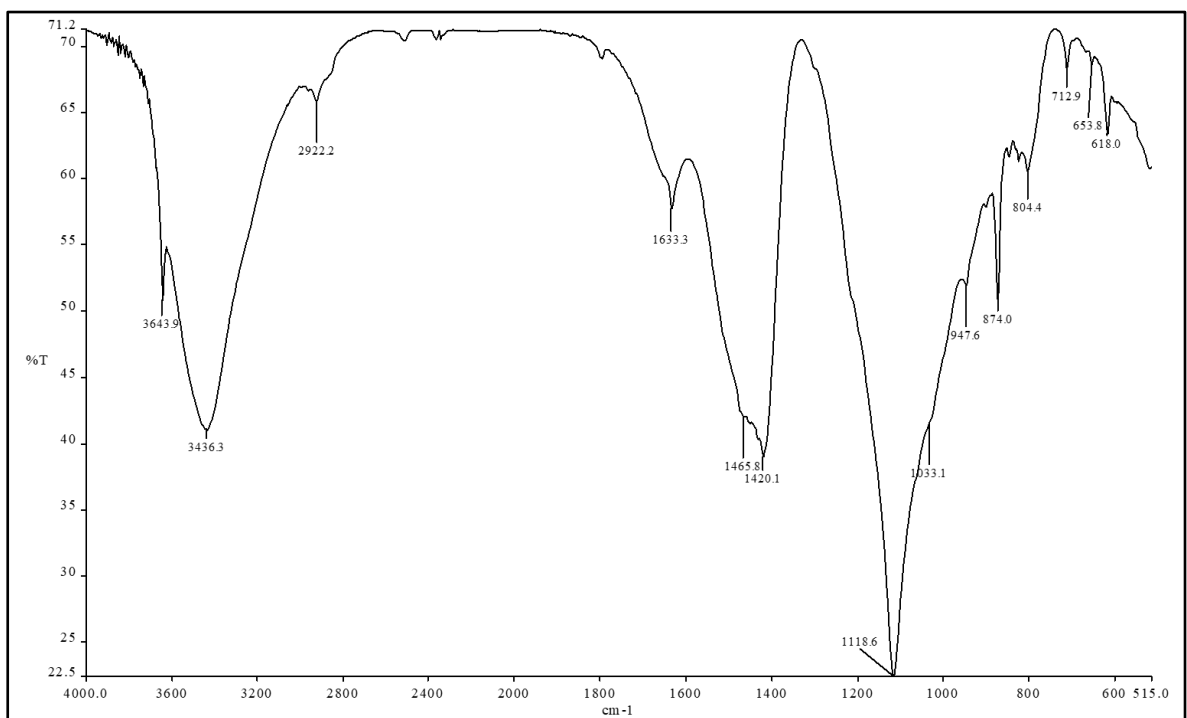

Figure 6: IR spectra of early hydration (1 day) of the NPB paste

4. Conclusion:

The hydration kinetics within the NPB has been analysed utilising analytical approach and compared with the reference cement. The sulphate activation of PSA particles by alkali sulphate rich fly ash was revealed in this analysis, where sulphate activation was found to be based on the reactivity of sulphates with the aluminium phase for producing ettringite (AFt). The ionic species of alkali sulphate (K^+, Na^+ and SO_4^{2-}) was found to influence the activation and subsequent hydration. During activation, the increased SO_4^{2-} concentration (from gypsum and alkali sulphate rich fly ash) reacts with alumina phase of PSA and forms aluminosulphate which combines with Ca^{2+} and forms ettringite. This ettringite contributes strength at an early stage [41-43]. At the same time the conversion of AFt to AFm phase was also confirmed by TG/DTA and FT-IR analysis during the progression of hydration within the novel NPB.

Due to creation of balanced oxide composition within the NPB, silica fume promotes pozzolanic reaction with calcium hydroxide and alkaline hydroxide and forms C-S-H. The progressive formation of C-S-H upon hydration was confirmed by both analysis. After 28 days of curing of NPB paste, C-S-H, the main strength generating phase was found to be reduced concentration in TG analysis. This observation was in accordance with the reduced rate of strength development in NPB mortar. However, the reduced density of the C-H phase after long term curing for successive Pozzolanic reaction within the ternary blend compared to the control cement was confirmed by TG/DTA and FT-IR. Moreover, consumption of Na^+, K^+ and OH^- ions as well as reduction of ion mobility in the pore solution, by silica fume, is expected to create a dense impermeable microstructure and control alkali silica reaction (ASR) and improve the soundness.

Reference:

1.   Filho, R.D.T., et al., *Potential for use of crushed waste calcined-clay brick as a supplementary cementitious material in Brazil.* Cement and Concrete Research, 2007. **37**(9): p. 1357-1365.

2.   Rodriguez Largo, O., et al., *Novel Use of Kaolin Wastes in Blended Cements.* Journal of the American Ceramic Society, 2009. **92**(10): p. 2443-2446.

3.   Erdem, T.K., et al., *Use of perlite as a pozzolanic addition in producing blended cements.* Cement & Concrete Composites, 2007. **29**(1): p. 13-21.

4.   Yilmaz, B. and N. Ediz, *The use of raw and calcined diatomite in cement production.* Cement & Concrete Composites, 2008. **30**(3): p. 202-211.

5.   Bertolini, L., et al., *MSWI ashes as mineral additions in concrete.* Cement and Concrete Research, 2004. **34**(10): p. 1899-1906.

6.   Lampris, C., J.A. Stegemann, and C.R. Cheeseman, *COMPARISON OF THE PHYSICAL PROPERTIES AND LEACHING CHARACTERISTICS OF APC RESIDUES SOLIDIFIED USING PORTLAND CEMENT AND GROUND GRANULATED BLAST FURNACE SLAG*, in *WASCON CONFERENCE*2009: France.

7.   Johnson, A., L.J.J. Catalan, and S.D. Kinrade, *Characterization and evaluation of fly-ash from co-combustion of lignite and wood pellets for use as cement admixture.* Fuel, 2010. **89**(10): p. 3042-3050.

8.   Udoeyo, F.F., et al., *Potential of wood waste ash as an additive in concrete.* Journal of Materials in Civil Engineering, 2006. **18**(4): p. 605-611.

9.   Adesanya, D.A. and A.A. Raheem, *Development of corn cob ash blended cement.* Construction and Building Materials, 2009. **23**(1): p. 347-352.

10.   Ganesan, K., K. Rajagopal, and K. Thangavel, *Rice husk ash blended cement: Assessment of optimal level of replacement for strength and permeability properties of concrete.* Construction and Building Materials, 2008. **22**(8): p. 1675-1683.

11.   Mozaffari, E., et al., *An investigation into the strength development of Wastepaper Sludge Ash blended with Ground Granulated Blastfurnace Slag.* Cement and Concrete Research, 2009. **39**(10): p. 942-949.

12.   Osborne, G.J., *Durability of Portland blast-furnace slag cement concrete.* Cement and Concrete Composites, 1999. **21**(1): p. 11-21.

13.   Grasserbauer, M., *Materials analysis in high technology — From analytical chemistry to analytical science.* TrAC Trends in Analytical Chemistry, 1989. **8**(6): p. 191.

14.   Scrivener, K., R. Snellings, and B. Lothenbach, *A Practical Guide to Microstructural Analysis of Cementitious Materials*2016: Taylor & Francis.

15.   Ramachandran, V.S., *4 - Thermal Analysis*, in *Handbook of Analytical Techniques in Concrete Science and Technology*, V.S. Ramachandran and J.B. James, Editors. 2001, William Andrew Publishing: Norwich, NY. p. 127-173.

16.   Odler, I., *Hydration, Setting and Hardening of Portland Cement*, in *Lea's Chemistry of Cement and Concrete (Fourth Edition)*, P.C. Hewlett, Editor 2003, Butterworth-Heinemann: Oxford. p. 241-297.

17.   Esteves, L.P., *On the hydration of water-entrained cement–silica systems: Combined SEM, XRD and thermal analysis in cement pastes.* Thermochimica Acta, 2011. **518**(1–2): p. 27-35.

18.   Fernández-Carrasco, L., et al., *Infrared Spectroscopy in the Analysis of Building and Construction Materials*, in *Infrared Spectroscopy - Materials Science, Engineering and Technology*, T. Theophile, Editor 2012, InTech.

19.   Mollah, M.Y.A., et al., *A Fourier transform infrared spectroscopic investigation of the early hydration of Portland cement and the influence of sodium lignosulfonate.* Cement and Concrete Research, 2000. **30**(2): p. 267-273.

20.   Kaminskas, R., J. Mituzas, and A. Kaminskas, *The effect of pozzolana on the properties of the finest fraction of separated Portland cement - part 1.* Ceramics-Silikaty, 2006. **50**(1): p. 15-21.

21.   Ylmén, R., et al., *Early hydration and setting of Portland cement monitored by IR, SEM and Vicat techniques.* Cement and Concrete Research, 2009. **39**(5): p. 433-439.

22.   Ashraf, M., et al., *Physico-chemical, morphological and thermal analysis for the combined pozzolanic activities of minerals additives.* Construction and Building Materials, 2009. **23**(6): p. 2207-2213.

23.   Singh, N.B., et al., *Effect of lignosulfonate, calcium chloride and their mixture on the hydration of RHA-blended portland cement.* Cement and Concrete Research, 2002. **32**(3): p. 387-392.

24.   Tkaczewska, E. and J. Małolepszy, *Hydration of coal–biomass fly ash cement.* Construction and Building Materials, 2009. **23**(7): p. 2694-2700.

25.   Pane, I. and W. Hansen, *Investigation of blended cement hydration by isothermal calorimetry and thermal analysis.* Cement and Concrete Research, 2005. **35**(6): p. 1155-1164.

26.   Rust, D., et al., *clinkerless cement produced from flue gas desulphurization residues and fly ash*, in *2009 World of coal ash (WOCA)*2009: Lexington, KY, USA.

27.   Marsh, B.K., R.L. Day, and D.G. Bonner, *STRENGTH GAIN AND CALCIUM HYDROXIDE DEPLETION IN HARDENED CEMENT PASTES CONTAINING FLY-ASH.* Magazine of Concrete Research, 1986. **38**(134): p. 23-29.

28.   Nithya, R., et al., *A Thermal Analysis Study on Blended Ternary Cement Paste.* International Journal of Chemistry, 2010. **2**(1).

29.   Trifunovic, P.D., et al., *The effect of the content of unburned carbon in bottom ash on its applicability for road construction.* Thermochimica Acta, 2010. **498**(1–2): p. 1-6.

30.   Dweck, J., et al., *Hydration of a Portland cement blended with calcium carbonate.* Thermochimica Acta, 2000. **346**(1–2): p. 105-113.

31.   Zingg, A., et al., *Interaction of polycarboxylate-based superplasticizers with cements containing different C3A amounts.* Cement and Concrete Composites, 2009. **31**(3): p. 153-162.

32.   Xiao, L. and Z. Li, *New Understanding of Cement Hydration Mechanism through Electrical Resistivity Measurement and Microstructure Investigations.* Journal of Materials in Civil Engineering, 2009. **21**(8): p. 368-373.

33.   Trifunovic, P.D., et al., *The effect of the content of unburned carbon in bottom ash on its applicability for road construction.* Thermochimica Acta, 2010. **498**(1-2): p. 1-6.

34.   Kourounis, S., et al., *Properties and hydration of blended cements with steelmaking slag.* Cement and Concrete Research, 2007. **37**(6): p. 815-822.

35.   Escalante-García, J.I., et al., *Fluorgypsum binders with OPC and PFA additions, strength and reactivity as a function of component proportioning and temperature.* Cement and Concrete Composites, 2008. **30**(2): p. 88-96.

36.   Katsioti, M., et al., *Properties and hydration of blended cements with mineral alunite.* Construction and Building Materials, 2009. **23**(2): p. 1011-1021.

37.   Fu, X.H., et al., *Studies on effects of activators on properties and mechanism of hydration of sulphoaluminate cement.* Cement and Concrete Research, 2003. **33**(3): p. 317-324.

38.   Taylor, H.F.W., *Hydration of Portland cement*, in *Cement Chemistry*, H.F.W. Taylor, Editor 1997, Thomas Telford: London.

39.   Ghosh, S.N., *5 - IR Spectroscopy*, in *Handbook of Analytical Techniques in Concrete Science and Technology*, V.S. Ramachandran and J.B. James, Editors. 2001, William Andrew Publishing: Norwich, NY. p. 174-204.

40.   Bensted, J. and S.P. Varma, *SOME APPLICATIONS OF INFRARED AND RAMAN SPECTROSCOPY IN CEMENT CHEMISTRY.* Cem Technol, 1974. **5**(4): p. 378-382.

41.   Qian, J.S., C.J. Shi, and Z. Wang, *Activation of blended cements containing fly ash.* Cement and Concrete Research, 2001. **31**(8): p. 1121-1127.

42.   Xu, A.M. and S.L. Sarkar, *Microstructural study of gypsum activated fly-ash hydration in cement paste.* Cement and Concrete Research, 1991. **21**(6): p. 1137-1147.

43.   Poon, C.S., et al., *Activation of fly ash/cement systems using calcium sulfate anhydrite (CaSO4).* Cement and Concrete Research, 2001. **31**(6): p. 873-881.